Heliyon 10 (2024) e33938

Contents lists available at ScienceDirect

Heliyon

journal homepage: www.cell.com/heliyon

Research article

MiR-30c suppresses the proliferation, metastasis and polarity reversal of tumor cell clusters by targeting MTDH in invasive micropapillary carcinoma of the breast

Yunwei Han [a,b,c,d,e,f,1], Weidong Li [a,b,c,d,e,f,1], Renyong zhi [a,b,c,d,e,f], Gui Ma [g,h,i], Ang Gao [g,h,i], Kailiang Wu [a,b,c,d,e,f], Hui Sun [a,b,c,d,e,f], Dan Zhao [g,h,i], Yiling Yang [a,b,c,d,e,f], Fangfang Liu [a,b,c,d,e,f], Feng Gu [a,b,c,d,e,f], Xiaojing Guo [a,b,c,d,e,f], Jintang Dong [g,h,i], Shuai Li [a,b,c,d,e,f,**], Li Fu [a,b,c,d,e,f,j,k,l,*]

[a] *Department of Breast Cancer Pathology and Research Laboratory, Tianjin Medical University Cancer Institute and Hospital, Tianjin 300060, China*
[b] *National Clinical Research Center of Cancer, Tianjin 300060, China*
[c] *Tianjin's Clinical Research Center for Cancer, Tianjin 300060, China*
[d] *Key Laboratory of Breast Cancer Prevention and Therapy, Tianjin Medical University, Tianjin 300060, China*
[e] *Ministry of Education, Breast Cancer Innovation Team of the Ministry of Education, Tianjin 300060, China*
[f] *Key Laboratory of Cancer Prevention and Therapy, State Key Laboratory of Breast Cancer Research, Tianjin 300060, China*
[g] *Department of Genetics and Cell Biology, College of Life Sciences, Nankai University, 94 Weijin Road, Tianjin 300071, China*
[h] *Southern University of Science and Technology, School of Medicine, 1088 Xueyuan Road, Shenzhen, Guangdong 518055, China*
[i] *Emory Winship Cancer Institute, Department of Hematology and Medical Oncology, Emory University School of Medicine, 1365C Clifton Road, Atlanta, 30322, Georgia, USA*
[j] *School of Life Science and Technology, ShanghaiTech University, Shanghai 201210, China*
[k] *Gene Editing Center, School of Life Science and Technology, ShanghaiTech University, Shanghai 201210, China*
[l] *Shanghai Institute for Advanced Immunochemical Studies, ShanghaiTech University, Shanghai 201210, China*

ARTICLE INFO

Keywords:
Breast cancer
Invasive micropapillary carcinoma (IMPC)
MiRNA
Proliferation

ABSTRACT

Purpose: Invasive micropapillary carcinoma (IMPC) of the breast has a high propensity for lymphovascular invasion and axillary lymph node metastasis and displays an 'inside-out' growth pattern, but the molecular mechanism of invasion, metastasis and cell polarity reversal in IMPC is unclear.

Methods: and Patients: Cell growth curves, tumor sphere formation assays, transwell assays, mouse xenograft model and immunofluorescence were evaluated to investigate the effects of miR-

Abbreviations: IMPC, Invasive micropapillary carcinoma; IDC-NST, Invasive ductal carcinoma no special type; ISH, *in-situ* hybridization; IHC, Immunohistochemistry; ER, Estrogen receptor; PR, Progestrone receptor; HER2, Human epidermal growth factor receptor 2; OS, Overall survival; DFS, Disease-free survival.

* Corresponding author. Department of Breast Pathology and Lab, Tianjin Medical University Cancer Institute and Hospital, National Clinical Research Center for Cancer, Key Laboratory of Cancer Prevention and Therapy, Ministry of Education, West Huanhu Road, Ti Yuan Bei, Hexi District, Tianjin 300060, China.

** Corresponding author. Department of Breast Pathology and Lab, Tianjin Medical University Cancer Institute and Hospital, National Clinical Research Center for Cancer, Key Laboratory of Cancer Prevention and Therapy, Ministry of Education, West Huanhu Road, Ti Yuan Bei, Hexi District, Tianjin 300060, China.

E-mail addresses: shuaili@tmu.edu.cn (S. Li), fuli@tijmu.edu.cn (L. Fu).

[1] These authors contributed equally to this work.

https://doi.org/10.1016/j.heliyon.2024.e33938
Received 21 January 2024; Received in revised form 30 June 2024; Accepted 1 July 2024
Available online 2 July 2024

Metastasis
Polarity reversal

30c and MTDH. Dual luciferase reporter assays was performed to confirm that the MTDH (metadherin) 3′UTR bound to miR-30c. MiRNA *in situ* hybridization (ISH) and immunohistochemistry (IHC) were carried out on IMPC patient tissues for miR-30c and MTDH expression, respectively. *Results:* We found miR-30c as a tumor suppressor gene in cell proliferation, metastasis and polarity reversal of IMPC. Overexpression of miR-30c inhibited cell growth and metastasis *in vitro* and *in vivo*. MiR-30c could directly target the MTDH 3′UTR. MiR-30c overexpression inhibited breast cancer cell proliferation, invasion and metastasis by targeting MTDH. Moreover, miR-30c/MTDH axis could also regulate cell polarity reversal of IMPC. By ISH and IHC analyses, miR-30c and MTDH were significantly correlated with tumor size, lymph nodule status and tumor grade, the 'inside-out' growth pattern, overall survival (OS) and disease-free survival (DFS) in IMPC patients.
Conclusions: Overall, miR-30c/MTDH axis was responsible for tumor proliferation, metastasis and polarity reversal. It may provide promising therapeutic targets and prognostic biomarkers for patients with IMPC.

1. Introduction

Invasive micropapillary carcinoma (IMPC) of the breast is an aggressive subtype of breast cancer (2019 WHO classification of breast cancer) characterized by small papillary structures lacking true central fibrovascular cores and special growth patterns of clusters of cells with reversed polarity [1,2]. This micropapillary growth pattern has also been identified in multiple tumor tissues, such as gastric [3], colon [4], and lung [5] and is associated with poor prognosis. Although the incidence of IMPC ranges from 2 to 8 % of all primary breast cancers, it exhibits more aggressive characteristics, such as lymphovascular invasion, lymph node metastasis, and distant metastasis [6–12]. Recently, the whole-genome sequencing of tumor cell clusters and spatial transcriptomics reveals gene expression characteristics of IMPC [13,14]. The precise pathologic diagnosis and individualized treatment have improved the outcomes of IMPC patients [15].

MicroRNA (miRNA), a kind of short noncoding RNA (ncRNA), plays vital regulatory roles in cell proliferation, differentiation, autophagy, apoptosis and senescence [16,17]. More than half of human miRNA genes are localized within fragile genomic regions, which are subject to different structural genomic alterations in cancer development [18]. The dysregulation of miRNA expression seems to be a hallmark of metastasis. MiR-10b overexpression could positively regulate cell migration and invasion by targeting the prometastatic gene RHOC [19]. The high levels of serum miR-103 could target multiple endothelial junction genes and promote tumor metastasis [20].miR-30c regulated invasion by targeting the cytoskeleton genes Twinfilin 1 and Vimentin, and regulated epithelial-to-mesenchymal transition (EMT) and chemo-resistance of breast tumor cells [21,22]. Our previous study showed that miR-30c was significantly downregulated in IMPC compared with IDC-NST (Invasive ductal carcinoma no special type) [23]. The potential role of miR-30c downregulation in IMPC needs to be further investigated.

The previously studies found MTDH as an important driver gene in poor-prognosis of breast cancer patients [24,25]. MTDH is also significant in tumor initiation, chemotherapy resistance and metastasis [24,26,27]. The whole body gene knockout studies of MTDH in prostate, liver, lung, and colorectal cancers had the similar results [26,28,29]. Our previous study showed high expression of MTDH is facilitates to lymph node metastasis of IMPC [30]. MTDH is also involved in cell polarity regulation and recruited during the maturation of the tight junction proteins ZO-1 and occludin in polarized epithelial cells [31].

In the current study, we found miR-30c could inhibit cell proliferation, invasion and metastasis both *in vitro* and *in vivo*. MiR-30c could directly target the MTDH 3′UTR and inhibit breast cancer cell proliferation, invasion and metastasis. MiR-30c negatively regulated MTDH, which may be involved in modifying the apico-basal polarity of IMPC. We also revealed that miR-30c and MTDH were significantly associated with multiple clinical pathological characteristics, prognosis and the 'inside-out' growth pattern of IMPC patients. These findings suggest that the miR-30c/MTDH axis plays an important role in proliferation, metastasis and the polarity reversal and may serve as prognostic markers of IMPC.

2. Materials and Methods

2.1. Clinical tumor specimens

Primary breast cancer specimens were obtained from the tissue bank at the Department of Breast Cancer Pathology and Research Laboratory, Tianjin Medical University Cancer Institute and Hospital, Tianjin, China. Formalin-fixed paraffin-embedded (FFPE) primary tumor specimens of IMPC (n = 124, from Jan 2007 to Dec 2012) and the period corresponding to IDC-NST (n = 149) were diagnosed by three independent pathologists. Patients who had received chemotherapy or radiation before surgery were eliminated, and their complete clinical data were available. According to the World Health Organization (WHO) classification, the histologic type determination was based on the tumor-node-metastasis (TNM) staging system. The overall survival (OS) and disease-free survival (DFS) rates were used to calculate. OS was defined as the time from diagnosis to the date of death. DFS was calculated from diagnosis to disease progression or death, regardless of which occurred first. In IMPC patients, the median follow-up was 72 months, recurrence or distant organ metastasis was observed in 33 patients, and 22 patients died. The studies were approved by an independent ethics committee of the Department of Breast Cancer Pathology and Research Laboratory, Tianjin Medical University Cancer Hospital,

Tianjin, China (Grant Nos. Ek2018136).

2.2. Cell lines and culture

The normal breast cell line MCF-10A and breast cancer cell lines (MCF-7, T47D, MDA-MB-231, BT-549, Hs-578T, HCC-1806), HEK293 and HEK293T cells were purchased from American Type Culture Collection (ATCC, Manassas, USA). As their phenotypic characteristics and patterns of genomic copy number variation (CNV) are consistent with those of the IMPC specimens [32], the breast cancer cell lines were used in this study. The breast cancer cells were cultured in DMEM high glucose (Gibco) with 10 % fetal bovine serum (Thermo Fisher Scientific, USA), 100 U/ml penicillin and 100 U/ml streptomycin (Gibco) at 37 °C in a 5 % CO_2 incubator. The medium was changed every 8 h. In primary breast cancer culture, the cells were treated as previously described [33].

2.3. miRNA in situ hybridization and protein immunohistochemical analysis

miRNA *in situ* hybridization (ISH) procedures were conducted as previously described [34]. Tumor sections were digested with proteinase K for 10 min and hybridized with hybridization solution at 54 °C for 2 h with double-DIG-LNA probes for miR-30c, U6 (positive control) or scrambled RNA (negative control) (Exiqon, Denmark) (Fig. S1). The slides were washed with PBS for three times, and incubated with sheep anti-DIG-AP (Roche, Switzerland) and then stained with nitroblue tetrazolium/5-bromo-4- chloro-3-indolyl-phosphate (Roche, Switzerland). Nuclear Fast Red was used to counterstain the nuclei. A positive signal appeared blue in the cytoplasm and nucleus. The intensities of miR-30c staining were scored as 0–4, according to previously described standards [35].

Immunohistochemical staining was performed on FFPE tissue sections. The sections were incubated with primary antibodies against MTDH (Invitrogen, catalogue # 40–6500, USA, 1:100), MUC1 (Abcam, catalogue # ab45167, England, 1:100), Vimentin (Cell Signaling Technology, catalogue # 3932, USA, 1:200), N-cadherin (BD Biosciences, catalogue # 610920, USA,1:200), E-cadherin (Cell Signaling Technology, catalogue # 3195, USA, 1:200), and Ki67 (Thermo Fisher Scientific, catalogue # RM9106S0, USA, 1:500) overnight at 4 °C. Then, the sections were treated with biotinylated antibody, streptavidin-biotin-peroxidase and DAB complex (Beijing Zhongshan Biotechnology, China). The nuclei were counterstained with hematoxylin. The intensities of MUC1 and MTDH staining were scored between 0 and 4 as previously described [36,37].

2.4. RNA isolation and quantitative real-time polymerase chain reaction (qRT-PCR)

Total RNA was extracted from breast cancer tissues (n = 12 per group) or cells with TRIzol reagents (Invitrogen, Carlsbad, CA, USA), according to the manufacturer's protocol. The Prime-Script RT reagent kit (TaKaRa, Shiga, Japan) was used to synthesize cDNA from mRNA. The realtime PCR was conducted with SYBR Premix Ex Taq (TaKaRa).The miRcute Plus miRNA First-Strand cDNA Synthesis Kit (KR211,Tiangen, China) was used to reverse transcribe miRNA. The realtime PCR was conducted with miRcute Plus miRNA qPCR Detection Kit (SYBR Green) (FP411,Tiangen, China). Results were analyzed with $2^{-\triangle\triangle CT}$ method, and GAPDH or U6 small RNA was used for normalization of MTDH or miR-30c, respectively. The primers were obtained from Tiangen (China): miR-30c (Forward, 5′- UGUAAACAUCCUACACUCU CAGC -3'; U6 (Forward, 5′-GCTTCGGCAGCACATATACTAAAA T-3'; Reverse, 5′-CGCTTCACGAATTTGCGTGTCAT-3′), MTDH (Forward, 5′- AAATGGGCGGACTGTTGAAGT -3'; Reverse, 5′- CTGTTTTGCACTGCTTT AGCAT -3′), GAPDH (Forward, 5′-GGTGGTCTCCTCTGACTTCAACA -3'; Reverse, 5′- GTTGCTGT AGCCAAATTCGTTGT-3′). The entire experiment was repeated three times.

2.5. Vector construction and lentivirus production

MTDH 3′UTR fragments containing miR-30c putative targeting sites were subcloned into the firefly luciferase 3′UTR. Point mutations of miR-30c targeting sites were generated by a plasmid site-directed mutagenesis kit (TaKaRa, Japan).

The pLKO.1-puro empty vector and plasmids containing shRNA against MTDH were purchased from Sigma. Lentiviral particles were produced in HEK293T cells by cotransfecting the cells with pLKO.1, pMD2.G and psPAX2 plasmids using Lipofectamine 2000 reagent (Invitrogen, CA) according to the manufacturer's protocol.

Cells were cultured in 24-well plates with a transfection complex. Approximately 5 μl of 20 μM chemically synthesized miR-30c mimic, miR-30c inhibitor or negative siRNA control was used. Ectopic expression of miR-30c, MTDH was achieved by infection with lentiviral solution (GenePharma, China) along with vector control lentiviral supernatant containing 5 μg/ml polybrene (Sigma, USA). After the cells reached 90 % confluency, 2 μg/ml puromycin (Sigma, USA) was added for 3–5 days to select stable overexpression cells. The stable cells were maintained in medium containing 1 μg/ml puromycin.

2.6. Western blots

Cells were washed with PBS three times, and the proteins were extracted according to the instructions, then separated by 10 % SDS PAGE electrophoresis and transferred to PVDF membranes (Millipore, USA). To block nonspecific binding, the membranes were incubated with 5 % skim milk at room temperature for 1 h. Then the membranes were incubated with an antiserum containing antibodies overnight at 4 °C against MTDH (Invitrogen, catalogue # 40–6500, USA, 1:1000), β-actin (Sigma-Aldrich, catalogue # A2228, USA, 1:1000). Western Bright ECL (Advansta, CA) was used following standard protocols, and blots were imaged with the ImageQuant LAS 4000 luminescent image analyzer (General Electric, CT).

2.7. Dual luciferase reporter assay

HEK293 cells seeded in 24-well plates were cotransfected with 500 ng firefly luciferase reporter vector containing the MTDH 3′UTR (named psiCHECK2-MTDH-3′UTR wt) or MTDH 3′UTR mutant (named psiCHECK2-MTDH-3′UTR mut) and 100 nM of negative control siRNA or miR-30c mimics in a final volume of 0.5 ml using Lipofectamine 2000 (Invitrogen, USA). After transfection for 48 h, the Firefly and Renilla luciferase activities were measured with dual luciferase assays (Promega, WI) consecutively in triplicate and at least three times.

2.8. SRB assay and colony formation assay

For the SRB assay, the transfected cells were plated into 24-well plates at 5×10^4 cells/well and cultured. Cells were then fixed and stained with sulforhodamine B (SRB). For the colony formation assay, 5000 transfected cells per well were seeded in 6-well plates. After fourteen days, colonies were fixed with 4 % paraformaldehyde and then dyed with crystal violet for 15 min.

2.9. Cell invasion and migration assay

According to the manufacturer's protocol, the migration and invasion assay was performed using a Transwell system (24-well, 8 μm pore size with polycarbonate membrane; Corning Costar, USA). The invasion assay was also performed with the polycarbonate membranes were coated with 50 μl growth factor-reduced Matrigel (BD Biosciences, USA) at 37 °C for 1 h. Then, 800 μl serum-containing (20 % FBS) medium in each well was added to the lower chamber. A total of 1×10^5 resuspended cells were added to the upper inserts with 100 μl serum-free medium. 48 h later, the remaining upper side cells of the transwell device were removed, and the invading cells at the bottom side were fixed with 4 % paraformaldehyde and stained with crystal violet.

For wound healing assays, transfected cells were grown in complete medium, and 10 μl pipette tips were used to create an artificial wound in 24-well plates. The cells were washed with PBS to remove debris. After cultured for 24 h, the wound healing was observed.

2.10. Mouse xenograft model

The animal experiment was supported by the Animal Care and Use Center of Nankai University, Tianjin, China. 17β-Estradiol pellets (0.72 mg, 90-day release; Innovative Research of America, FL) were implanted subcutaneously in the shoulder region of each 4-week-old female BALB/c nude mouse (Charles River, China) one day before cell inoculation. MCF-7 cells (1×10^7) transfected with lenti-miR-30c or lenti-empty were resuspended in a solution of Matrigel (BD Biosciences, USA) or PBS (equal volume), respectively, and then inoculated subcutaneously into the flanks of BALB/c nude mice. Tumor volumes were measured once a week and calculated as follows: $A \times B^2/2$, where A is the largest diameter and B is the diameter perpendicular to A. After eight weeks, mice were sacrificed and tumors were removed. Then the tumors were weighed, and fixed in 4 % formalin for 48 h. H&E staining was used for histological examination.

To evaluate the effect of miR-30c on tumor metastasis, 1×10^6 MDA-MB-231 cells infected with lenti-miR-30c or lenti-empty were injected into the tail veins of four-week-old female BALB/c nude mice (seven mice for each group). Four weeks later, the numbers of micrometastases in the lung per H&E stained section were analyzed for histological examination.

2.11. Three-dimensional (3D) morphogenesis assays

A three-dimensional (3D) morphogenesis assay was performed as previously described [38]. 50 μl of growth factor-reduced Matrigel (BD Biosciences, CA) were added to the eight-well chamber slides. After 1 h, a total of 5000 treated cells/well were overlaid onto the gel in DMEM supplemented with 10 % FBS and 2 % Matrigel and cultured for two weeks for counting using an inverted microscope. The three-dimensional culture Images were determined by the covered area of each sphere, and diameter of spheres were determined by the circle formula under a phase contrast microscope. Smaller spheres (less than 40 mm) were excluded. Experiments were repeated a minimum of three times.

For the three-dimensional (3D) morphogenesis assays assessment of breast cancer primary cell, after digested and centrifuged, the cells with a density of 1.5×10^5/ml were embedded in collagen gel in a 24-well plate. The complete medium was changed every 3 days. Then, the spheroids were harvested and counted after 3–7 days. The lenti-miR-30c or lenti-empty was added on the day of planting (according to the GenePharma lentiviral solution instructions).

2.12. Immunofluorescence analysis

Immunofluorescence analysis was performed as previously described [26].4 % paraformaldehyde for 20 min and washed with PBS for three times. After added 0.25 % Triton X-100 to the well for 20 min, the Collagen gel was blocked with 3 % bovine serum albumin for 40 min. After washed with PBS for three times, the cells were incubated in a darkroom at 4 °C overnight with a primary antibody, MUC-1 (1:2000, Abcam ab45167, England), and incubated at room temperature for 2 h with a secondary antibody. After washed with PBS for three times, the nucleus is dyed with DAPI (blue). The spheroids of 'inside-out' staining pattern of MUC1 were harvested and counted by morphological observation. The immunofluorescent images were observed by the Olympus IX51 (Olympus, Tokyo, Japan) confocal microscope.

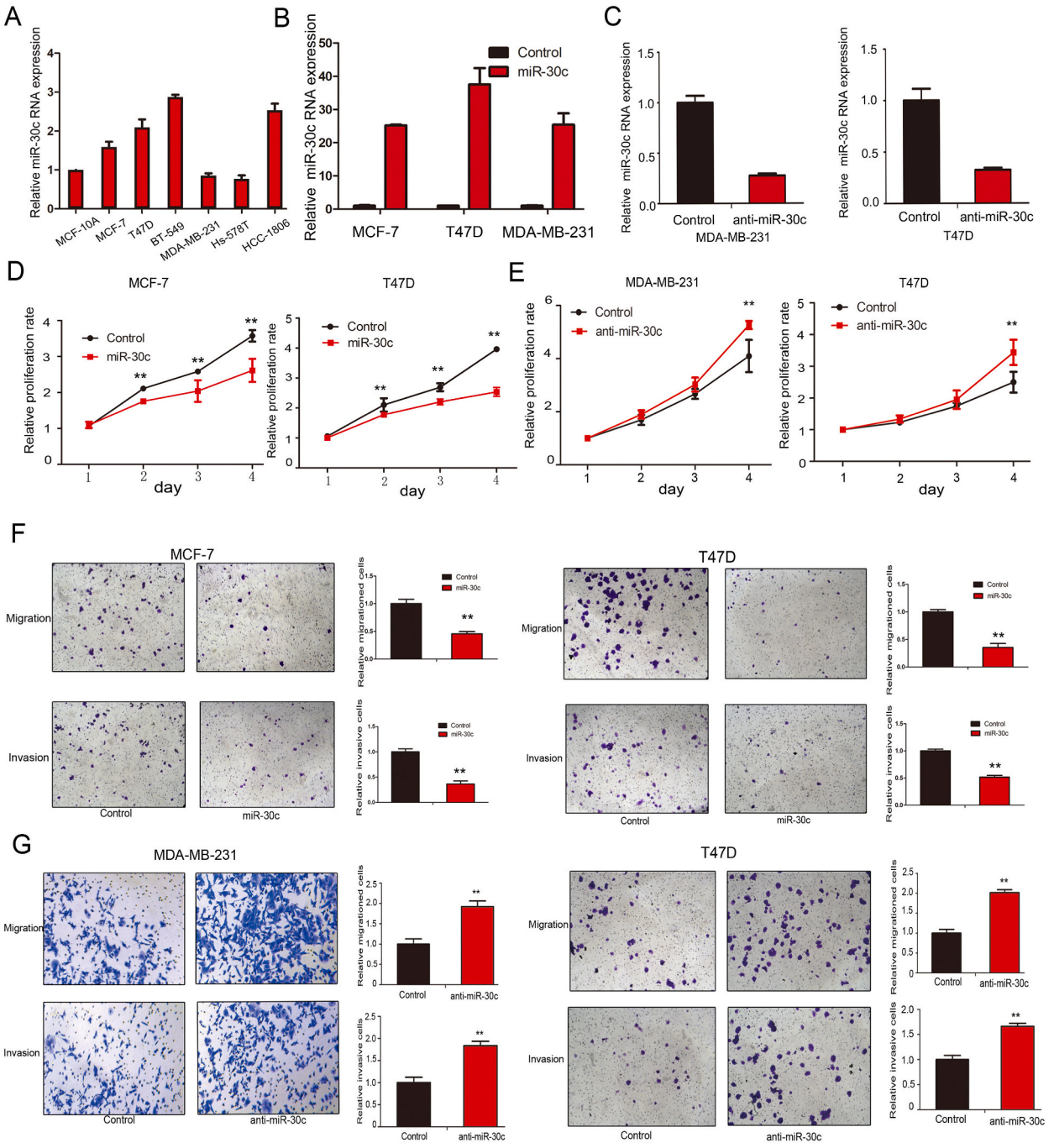

Fig. 1. MiR-30c overexpression inhibits the cell proliferation, migration and invasion *in vitro*. (A) Relative miR-30c expression levels in the normal breast cell line and six breast cancer cell lines were examined by quantitative real-time PCR (qPCR) assay, while U6 was used as an endogenous control for miRNA expression analysis. (B) The overexpression of miR-30c in MCF-7, T47D and MDA-MB-231 cells were validated by qPCR. (C)The down expression of miR-30c in MDA-MB-231and T47D cells was validated by qPCR. (D) Growth curves are presented after MCF-7 and T47D were transfected with miR-30c mimics or negative control. Cell growth was quantified and normalized to that at day 1. (E) Growth curves are presented after MDA-MB-231and T47D cells were transfected with miR-30c inhibitors or negative control. The growth of cells was quantified and normalized to that at day 1. (F) Transwell assays were performed to examine the migration and invasion abilities of MCF-7 and T47D cells transfected with miR-30c mimics or negative control. The relative migration and invasion abilities of MCF-7 and T47D cells were analyzed quantitatively. (G) Transwell assays were performed to examine the migration and invasion ability of MDA-MB-231 cells and T47D cells transfected with miR-30c inhibitors or negative control. The relative migration abilities of MDA-MB-231 cells and T47D cells were analyzed quantitatively. Columns, average of at least three biological repeats; bars represent s. d.; *$p < 0.05$; **$p < 0.01$.

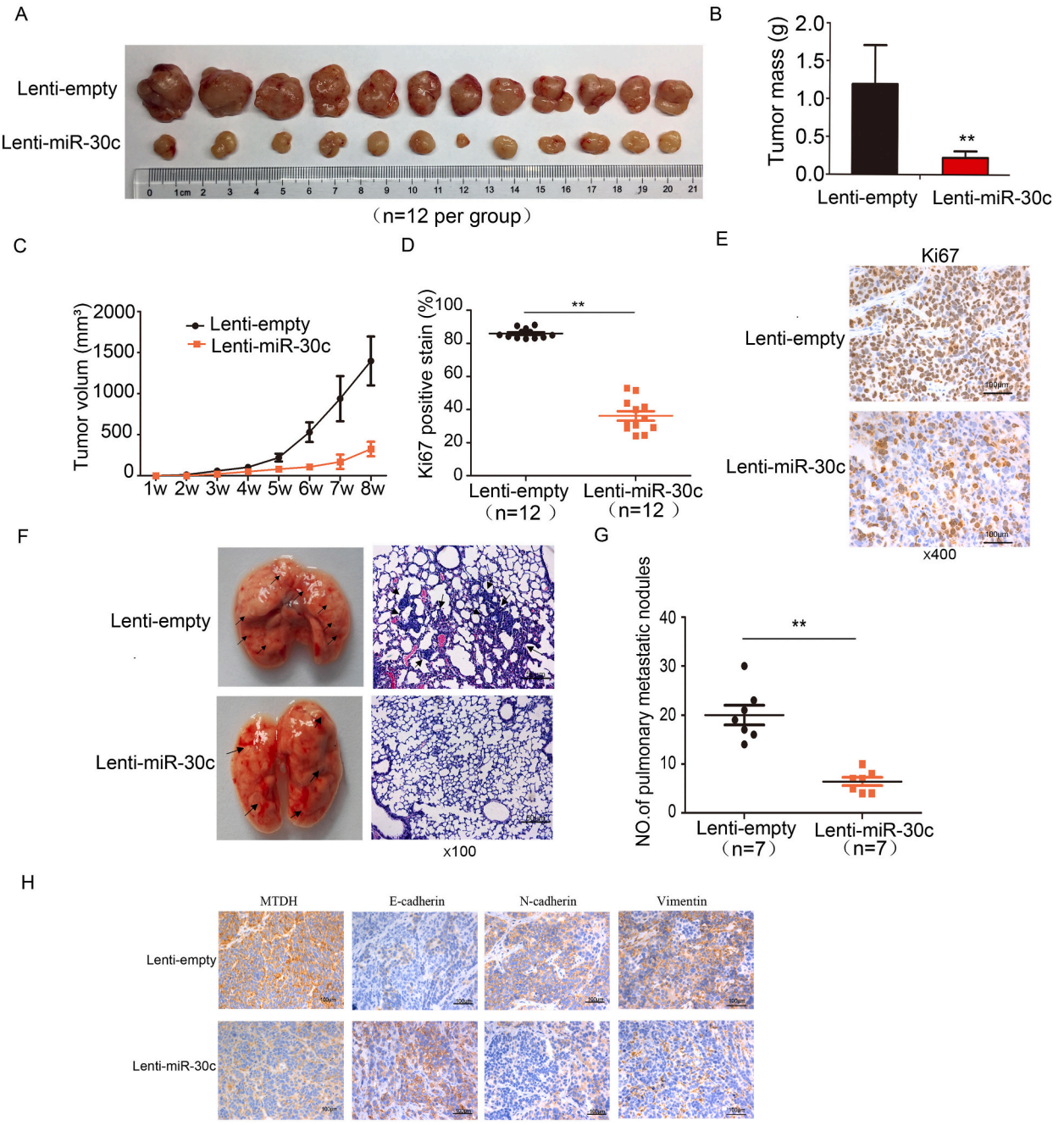

Fig. 2. MiR-30c inhibits tumorigenesis and metastasis *in vivo*. (A) MCF-7 cells transfected with lenti-miR-30c or lenti-empty were inoculated subcutaneously into the flanks of BALB/c female mice (n = 12), as described in the Materials and Methods. (B) Sixty days after injection, the mice were sacrificed, necropsies were performed, and the tumors were weighed. (C) The size of tumors in the two groups was measured and calculated and compared every week. (D, E) Histological examination of the tumor xenografts. Immunohistochemical analysis revealed Ki67 expression in xenografts (magnification at 400 ×). (F) MDA-MB-231 cells with lenti-miR-30c or lenti-empty were injected into the tail veins of nude mice (n = 7 per group). Four weeks after injection, mice were sacrificed. The numbers of pulmonary metastatic nodules in the lung were counted and compared with Student's t-test. Representative images of lung metastasis in each group (left). The micrometastases of the two groups in the lung per H&E stained section from individual mice were present (right). (G) The numbers of pulmonary metastatic nodules in each group were calculated and compared. (H) IHC analysis shows the expression of MTDH, E-cadherin, N-cadherin, Vimentin in xenografts (magnification at 400 ×). Columns, average of at least three biological repeats; bars represent s. d.; *$p < 0.05$; **$p < 0.01$.

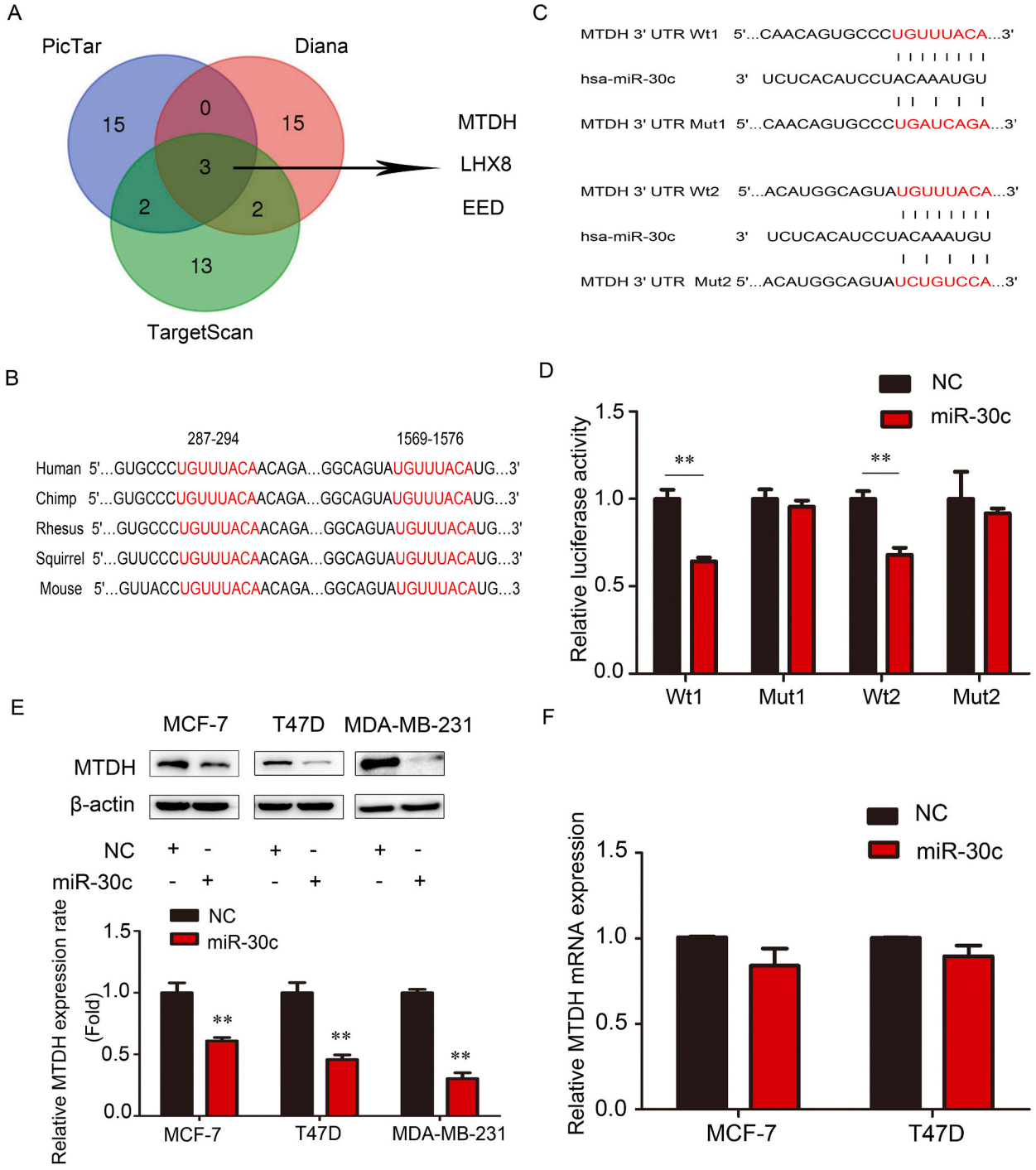

Fig. 3. MiR-30c inhibits MTDH expression by directly targeting its 3′UTR. (A) MiR-30c target genes were predicted by TargetScan, PicTar and DIANA algorithms. The overlapping genes were MTDH, LHX8, and EED. (B) The alignment of miR-30c target sequences in the MTDH 3′UTR from five mammals. The evolutionarily conserved nucleotides are highlighted in red. (C) Two predicted miR-30c target sites reside at nucleotides 287–294 and 1569–1576 of the MTDH 3′UTR; Wt: wild type, Mut: mutant. (D) Relative luciferase activity was analyzed after the Wt or Mut reporter plasmids were cotransfected into HEK293 cells with miR-30c mimics or negative control. (E) Western blot analysis of MTDH protein levels in MCF-7, T47D, MDA-MB-231 cells transfected with miR-30c mimics (20 μM, 5 μl) or negative control. Relative expression level was defined as the ratio between the gray value of MTDH and β-actin. (F) Relative MTDH mRNA levels were determined by quantitative real-time PCR (qPCR). GAPDH was used as the endogenous control for MTDH mRNA level analysis. Columns, average of at least three biological repeats; bars, s. d.; *$p < 0.05$; **$p < 0.01$. (For interpretation of the references to color in this figure legend, the reader is referred to the Web version of this article.)

2.13. Image analysis

To quantitate spheroids polarity, spheroids were stained for MUC1, and nuclei and analyzed with a confocal microscope. Spheroids with MUC1 staining at the interior were identified as spheroids with normal polarity (interior apical pole). Spheroids in IMPC with MUC1 staining at the surface (basal pole) and in which was absent from the interior apical pole were considered as inverted polarity. The spheroids of 'inside-out' staining pattern of MUC1 were counted by morphological observation and calculated as follows: the ratio = A/B, where A is the'inside-out' staining spheroids and B is the total spheroids [39,40]. The Smaller spheroids (less than 40 mm) were excluded. Experiments were repeated at least three times.

2.14. Statistics

Statistical analyses were performed using GraphPad Prism 5 software (GraphPad, CA) and the SPSS 21.0 software package (SPSS Inc, USA). Clinicopathological variables between the IMPC and IDC-NST groups were analyzed using the Chi-square test. Correlations between miR-30c, MTDH or MUC1 expression and clinicopathological variables were evaluated by Mann-Whitney *U* test and Spearman's rank correlation analysis. The Kaplan-Meier analysis was used to estimate OS and DFS rates. The relevant prognostic factors were determined by the Cox proportional risk regression analysis. Student's *t*-test was used for experimental quantitative analysis between the two groups. The statistical analysis was two-sided, and p-values less than 0.05 were considered statistically significant.

3. Results

3.1. MiR-30c overexpression inhibits the cell proliferation, migration and invasion in vitro

We examined the expression of miR-30c in the normal breast cell line and a series of breast cancer cell lines (Fig. 1A). Quantitative real-time PCR demonstrated that miR-30c mimics or inhibitors could efficiently regulate miR-30c by transfection in MCF-7, T47D and MDA-MB-231 cells (Fig. 1B and C). , We applied the SRB assay to examine of the effect of miR-30c regulation in cell growth ability. The overexpression of miR-30c was able to suppress cell proliferation in *vitro* significantly (Fig. 1D). We also adopted the colony formation and the three-dimensional (3D) morphogenesis assay to evaluate its oncogenic ability. As shown in Fig. S2A-B, overexpression of miR-30c exhibited reduced cologinic ability and inhibited tumorsphere formation in breast cancer cells. Moreover, we used miR-30c inhibitors to abrogate miR-30c expression in MDA-MB-231 and T47D cells. As expected, anti-miR-30c significantly induced cell proliferation ability (Fig. 1E).

To further explore the role of miR-30c in invasive behaviors *in vitro*, we used the transwell assay to detect the migration and invasion ability after miR-30c overexpression. As shown in Fig. 1F, miR-30c overexpression could potentially suppress migration and invasion of MCF-7 and T47D cell lines. Quantitative analysis showed on the right panel. As expected, anti-miR-30c significantly induced cell invasion and metastasis ability (Fig. 1G).These results indicated that ectopic expression of miR-30c suppressed cell proliferation, invasion and metastasis *in vitro*.

3.2. MiR-30c suppresses tumorigenesis and metastasis in a xenograft model

To further study the role of miR-30c in tumorigenesis *in vivo*, 1×10^7 MCF-7 cells infected with lenti-miR-30c or lenti-empty were inoculated subcutaneously into the flanks of twelve mice. Tumor volume was observed every week, and tumor growth curves were plotted. Lentivirus-mediated miR-30c overexpression significantly inhibited the tumor volume and weight compared with that in the lenti-empty group (Fig. 2A–C).

As indicated by Ki67 immunostaining, lenti-miR-30c significantly inhibited cell proliferation compared with that in the lenti-empty group *in vivo* (Fig. 2D and E).

To determine the role of miR-30c in breast cancer cell lung metastases, MDA-MB-231 cells were infected with lenti-miRNA-30c or lenti-empty and then tail vein injected. Four weeks after injection, mice were sacrificed, and lung metastasis was investigated. As shown in Fig. 2F and G, pulmonary metastatic nodules were reduced in the lenti-miR-30c group compared with the lenti-empty group. According to these results, enhanced expression of miR-30c decreased the tumorigenesis and metastasis *in vivo*. In addition, immunohistochemistry and Western blot analyses revealed that E-cadherin expression levels were upregulated and N-cadherin, Vimentin expression levels were downregulated in the lenti-miR-30c group compared with the lenti-empty group, indicating that miR-30c overexpression might inhibit the process of EMT (Fig. 2H, Fig.S3A).

3.3. MiR-30c inhibits MTDH expression by directly targeting its 3′UTR

Our previous research revealed that miR-30c was significantly downregulated in IMPC compared with IDC-NST [23]· To explore the downstream targets of miR-30c, we employed TargetScan, PicTar and DIANA bioinformatic tools to predict the target genes of miR-30c. As shown in Fig. 3A, three genes were predicted as a miR-30c target by the three different algorithms. Among the 3 genes, MTDH have revealed its crucial metastatic role in the metastatic ability of IMPC as our previous studies [30]. Moreover, 3′UTR of MTDH contain the two predicted target sites located at 287–294 nt and 1569–1576 nt were conserved among vertebrates (Fig. 3B). As indicated in Fig. 3C, two MTDH 3′UTR fragments containing the putative target sites and the corresponding mutant vectors with

several nucleotide substitutions were subcloned into the 3′UTR of the luciferase expression vector. As shown in Fig. 3D, miR-30c overexpression significantly downregulated luciferase activity in both reporter assays. Point mutations that interrupt base pairing between the miR-30c seed sequence and MTDH 3′UTR could block the inhibitory effect of miR-30c. MiR-30c overexpression could downregulate the protein levels of MTDH and anti-miR-30c significantly increased the protein levels of MTDH (Fig. 3E–S3B). However, miR-30c mimics slightly inhibiting MTDH mRNA levels (Fig. 3F). This is consistent with the common view that mammalian miRNAs mainly regulate gene expression through translational inhibition. All these results demonstrated that miR-30c regulated MTDH through direct binding to its 3′UTR.

3.4. MiR-30c inhibits breast cancer cell proliferation, migration and invasion by targeting MTDH

We examined MTDH knockdown could significantly inhibited tumor sphere formation in breast cancer cells (Fig.S3C). To further determine whether miR-30c exerts its function by inhibiting MTDH, we investigated the effects of miR-30c when MTDH was overexpressed. LV6-MTDH was introduced into MCF-7 and T47D cells to establish stable MTDH overexpression cells. Next, we re-expressed miR-30c in LV6-vector and LV6-MTDH cells (Fig. 4A). Relative expression rate of western blotting assay was showed in Fig.S3D. The

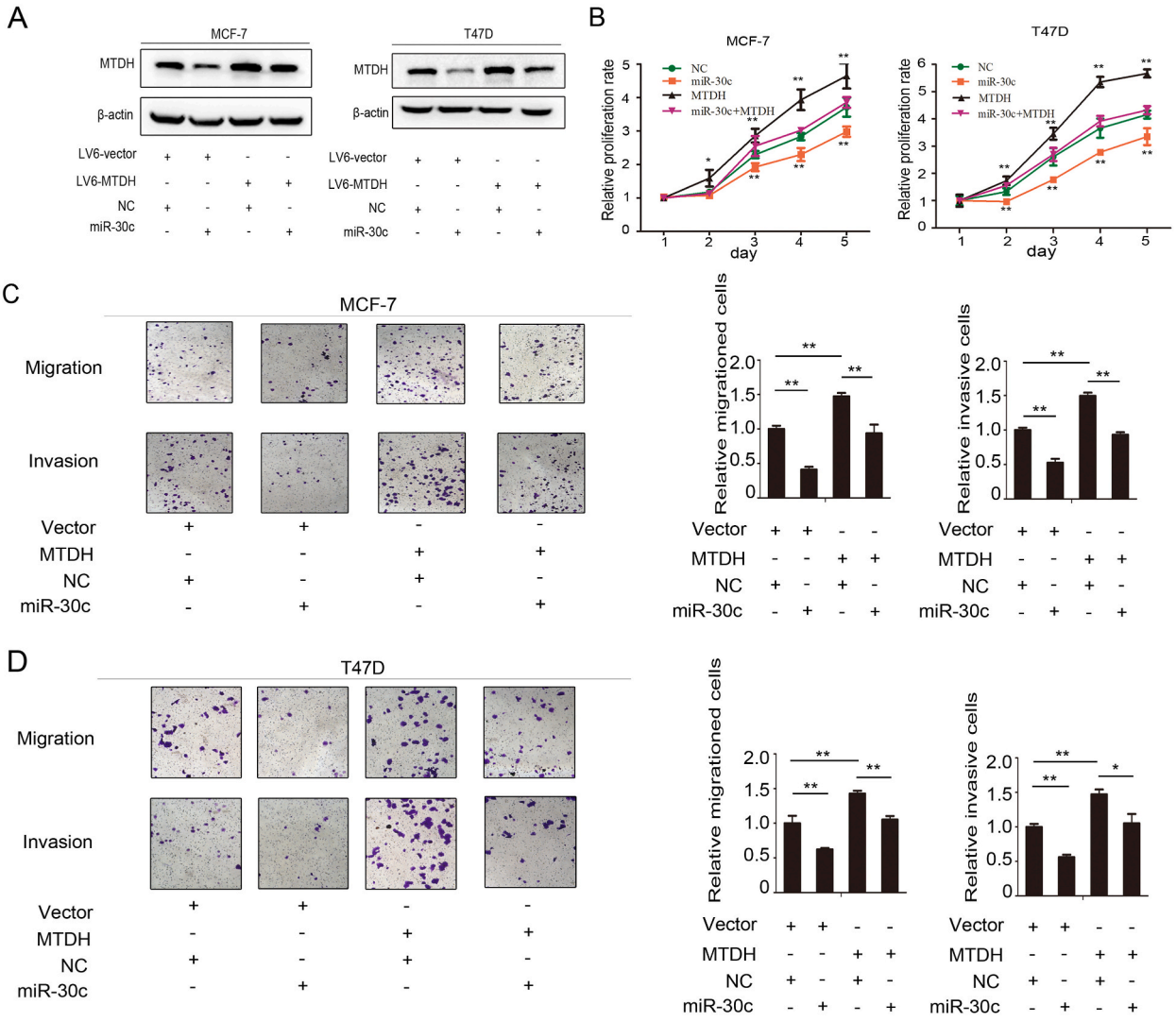

Fig. 4. MiR-30c inhibits breast cancer cell proliferation, migration and invasion by targeting MTDH. (A) Western blotting assay of MTDH are presented after MCF-7 and T47D cells were transfected with miR-30c mimics or negative control together with either LV6-MTDH or LV6-vector. β-actin was used as the endogenous control. (B) Growth curves are presented after MCF-7 and T47D cells were transfected with miR-30c mimics or negative control together with either LV6-MTDH or LV6-vector. Cell growth was quantified and normalized to that at day 1. (C, D) Transwell assays were performed to examine the migration and invasion abilities of MCF-7 and T47D cells transfected with miR-30c mimics or negative control together with either LV6-MTDH or LV6-vector. The relative migration and invasion abilities of MCF-7 and T47D cells were analyzed quantitatively. Columns, average of at least three biological repeats; bars, s. d. *$p < 0.05$; **$p < 0.01$.

results showed that overexpression of miR-30c significantly promoted proliferation ability of the cells, while overexpression of MTDH reversed such an effect partially ($p < 0.05$, Fig. 4B).

We examined whether miR-30c regulated cell migration and invasion via targeting MTDH. As shown in Fig. 4C-D, MTDH overexpression could rescue the inhibitory effects of miR-30c overexpression on migration and invasion. Quantitative analysis showed on the right panel. All these observations demonstrated that MTDH is a direct functional target of miR-30c.

3.5. MiR-30c regulates the polarity reversal of tumor cell clusters in IMPC by targeting MTDH

Mucin glycoproteins promote proliferation, invasion, and regulate cell polarity through diverse pathways in epithelial cancers [41]. Since the morphological characterization of IMPC can be assessed by the 'inside-out' staining pattern of epithelial membrane antigen (MUC1), we hypothesized that the miR-30c/MTDH axis might regulate the 'inside-out' growth pattern of IMPC. Quantitative real-time PCR and Western blot showed miR-30c mimics could overexpress miR-30c efficiently and downregulated the protein levels of MTDH in IMPC primary cells (Fig. 5A and B).To further analyze the role of the miR-30c/MTDH axis in cell polarity, IMPC primary cells were used for polarity studies *in vitro*. The results showed that miR-30c overexpression could decrease the spheroids of the 'inside-out' staining pattern of MUC1, and LV6-MTDH overexpression could increase the spheroids of the 'inside-out' staining pattern of MUC1. MTDH overexpression rescued the inhibitory effects of miR-30c overexpression on the spheroids of the inside-out staining pattern of MUC1, as demonstrated by multidimensional invasive spherical mass analysis (Fig. 5C and D). Our results indicate that miR-30c negatively regulates the polarity reversal of tumor cell clusters in IMPC by targeting MTDH, but there is not a strong overlapping localization between MTDH and MUC1 observed in confocal images of immunofluorescence in IMPC primary cells (Fig.S4).

3.6. MiR-30c/MTDH is correlated with the clinicopathologic characteristics and prognosis of IMPC

To explore miR-30c and MTDH expression in IMPC, we measured miR-30c and MTDH levels in 124 IMPC tissues and corresponding 149 IDC-NST tissues by ISH and IHC. Representative images of miR-30c, MTDH and MUC1 expression in IMPC and IDC-NST are shown in Fig. 6A and B, demonstrating that miR-30c expression was remarkably downregulated in IMPC tissues compared with IDC-NST tissues (0.78 *vs* 0.62, $p < 0.05$) (Table S1). Furthermore, we compared the expression levels of miR-30c between IMPC and IDC-

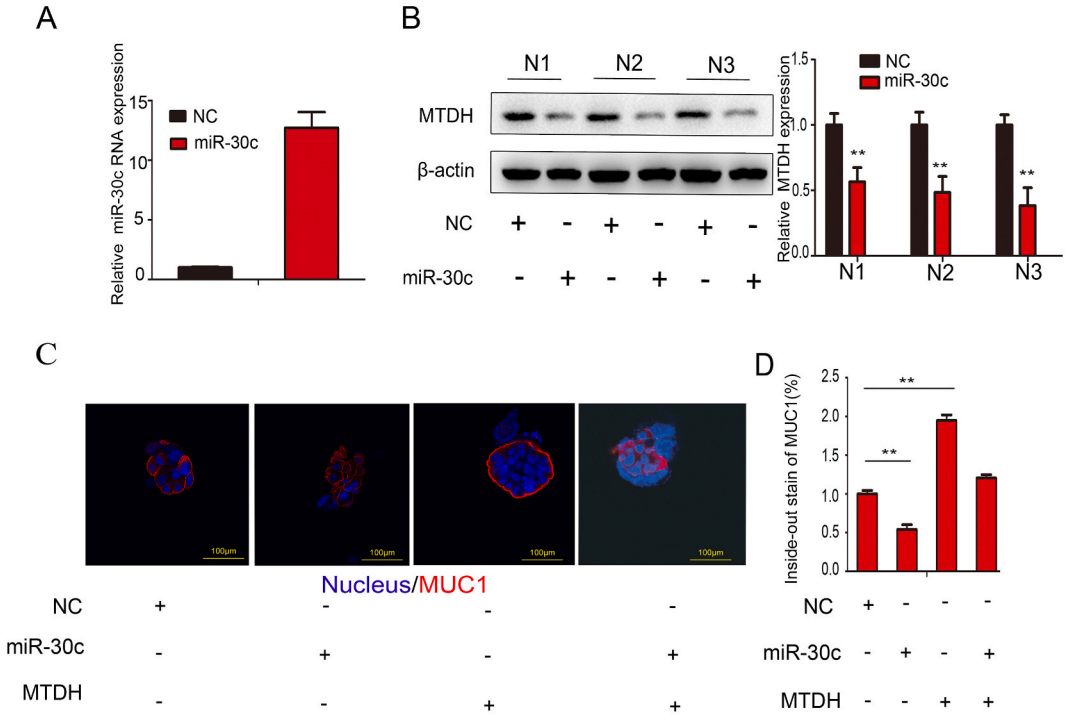

Fig. 5. MiR-30c regulates the polarity reversal of tumor cell clusters in IMPC by targeting MTDH. (A) The overexpression of miR-30c in IMPC primary cells was validated by qPCR. (B) Western blot analysis of MTDH protein levels in IMPC primary cells transfected with miR-30c mimics (20 μM, 5 μl) or negative control. Relative expression level was defined as the ratio between the gray value of MTDH and β-actin. (C) Immunofluorescence image of the inside-out staining pattern of MUC1 in LV6-vector and LV6-MTDH IMPC primary cells transduced by negative control or miR-30c mimics. (D) The spheroids of the inside-out staining pattern of MUC1 were analyzed quantitatively in LV6-vector and LV6-MTDH IMPC primary cells transduced by negative control or miR-30c mimics. Columns, average of at least three biological repeats; bars represent s. d.; *$p < 0.05$; **$p < 0.01$.

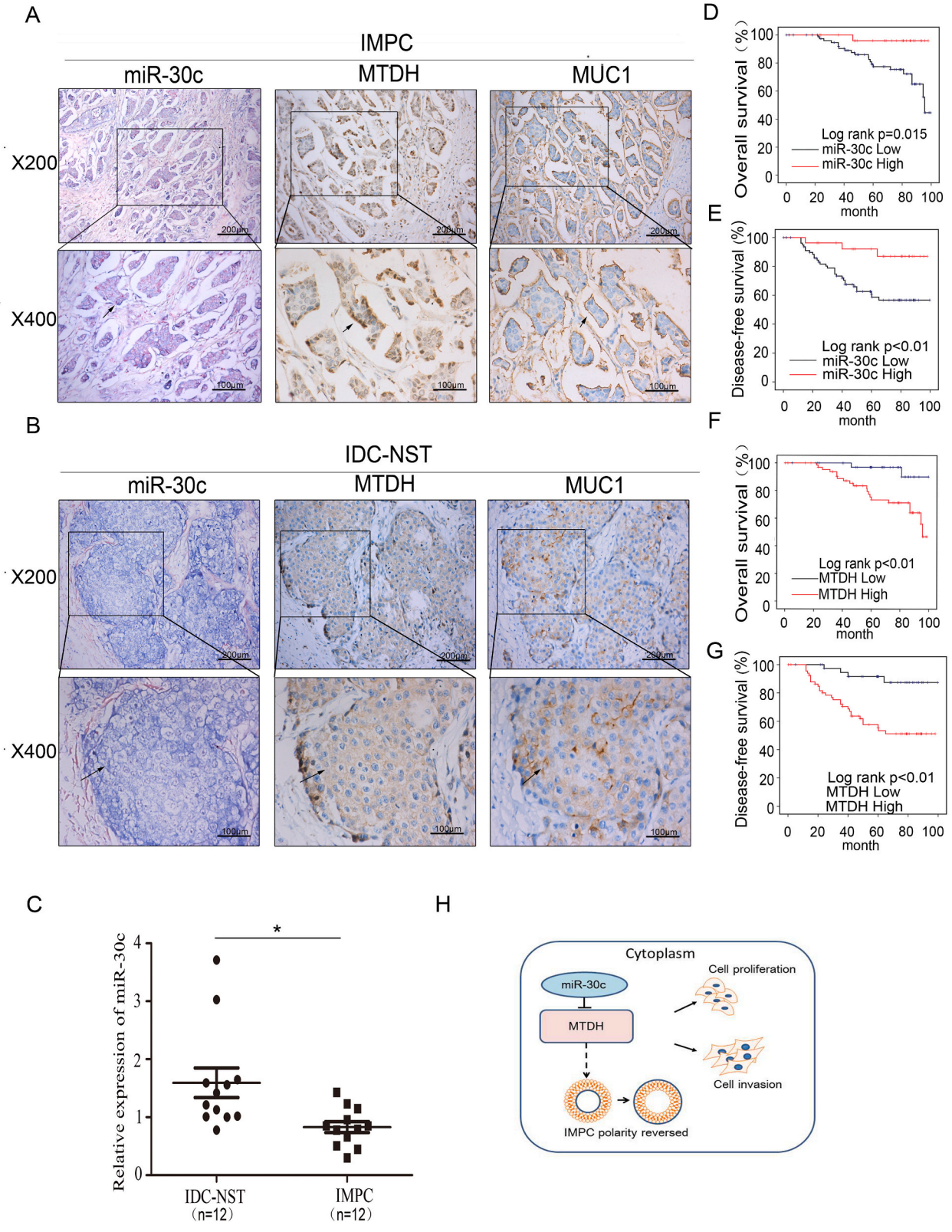

(caption on next page)

Fig. 6. MiR-30c/MTDH is correlated with the clinicopathologic characteristics and prognosis of IMPC. The miR-30c expression levels were analyzed in IMPC and IDC-NST tissues by *in situ* hybridization (ISH). MTDH and MUC1 expression levels were analyzed in IMPC and IDC-NST tissues by immunohistochemistry (IHC). (A, B) Representative images of miR-30c, MTDH and MUC1 expression in IMPC and IDC-NST tissues. (C) QPCR analysis shows the expression levels of miR-30c in 12 pairs of tissues. Expression for the gene was normalized to U6 expression. $^{*}p < 0.05$. (D, E) The overall survival and disease-free survival of patients with high or low miR-30c expression in IMPC patients. (F, G) The overall survival and disease-free survival of patients with high or low MTDH expression in IMPC patients. (H) A schematic showing how the signaling pathway of miR-30c regulates tumor cell invasion, metastasis and polarity reversal in invasive micropapillary carcinoma of the breast.

NST paired tissues by quantitative real-time PCR (n = 12). The results showed that the expression of miR-30c was downregulated in IMPC tissues compared with IDC-NST tissues (Student's t-test, $p < 0.05$, Fig. 6C). MTDH expression was significantly upregulated in IMPC tissues compared with IDC-NST tissues (0.64 *vs* 0.51, $p < 0.05$) (Table S1). Low expression levels of miR-30c were correlated with larger tumor size, multiple lymph node metastases, higher tumor grade and higher histologic grade ($p = 0.042$, $p < 0.01$, $p < 0.01$ and $p = 0.013$, respectively; Table 1). The MTDH levels were significantly higher in IMPC tissues, and the high expression of MTDH was correlated with large tumor size, multiple lymph node metastases and higher tumor grade ($p = 0.038$, $p < 0.01$ and $p < 0.01$, respectively; Table 1). To further study the association between miR-30c and MTDH expression, correlation analysis revealed that miR-30c was negatively correlated with MTDH in IMPCs (Table 2). The polarity reversal phenotype of MUC1 was negatively correlated with the miR-30c level and positively correlated with the MTDH expression level in IMPC patients (Table 2). These data indicated miR-30c reduction might contribute to the MTDH overexpression and lead to the polarity reversal of tumor cell clusters in IMPC.

Survival analysis showed IMPC patients with high miR-30c expression had better OS and DFS than patients with low miR-30c expression ($p = 0.015$ and $p < 0.01$, respectively; Fig. 6D and E). OS and DFS were better in IMPC patients with low MTDH expression than high MTDH expression ($p < 0.01$ and $p < 0.01$, respectively; Fig. 6F and G). Univariate and multivariate survival analyses for OS and DFS were also performed. Tumor stage ($p = 0.043$) and MTDH ($p = 0.028$) expression were independent risk factors for OS in IMPC (Table S2). Nodal stage ($p = 0.026$) and MTDH ($p = 0.01$) expression were independent risk factors for DFS in IMPC (Table S3). The results implicated a potential relationship between miR-30c and MTDH in the metastasis and prognosis of IMPC patients. Altogether, our results indicated that the miR-30c/MTDH axis might be important in the proliferation, metastasis and polarity reversal of tumor cell clusters of IMPC (Fig. 6H).

Table 1
Relationships between miR-30c and MTDH expression and clinicopathologics in IMPC patients.

Characteristic	miR-30c expression		z	*p*-value	MTDH expression		z	*p*-value
	High	Low			High	Low		
Age (years)			−0.424	0.671			−0.321	0.748
≥55	12	50			40	22		
< 55	15	47			40	22		
Tumor stage			−2.037	0.042			−2.075	0.038
T1 - T2	25	72			58	39		
T3 - T4	2	25			22	5		
Nodal stage			−3.296	<0.01			−3.461	<0.01
N0	10	8			8	10		
N1	6	24			15	15		
N2	6	21			17	10		
N3	5	44			40	9		
Grade			−3.268	<0.01			−2.925	<0.01
I	10	6			7	9		
II	7	29			19	17		
III-IV	10	62			54	18		
Histologic grade			−2.493	0.013			−0.506	0.613
1	14	26			25	15		
2	11	53			41	23		
3	2	18			14	6		
ER			−0.664	0.507			−0.589	0.556
Negative	9	26			24	11		
Positive	18	71			56	33		
PR			−0.427	0.669			−0.179	0.858
Negative	8	33			26	15		
Positive	19	64			54	29		
HER2			−0.488	0.626			−0.758	0.448
Negative	23	86			69	40		
Positive	4	11			11	4		
Subtype			−0.941	0.347			−1.135	0.256
ER/PR + HER2-	22	72			58	36		
ER/PR + HER2+	2	6			6	2		
ER/PR-HER2+	2	5			5	2		
Triple negative	1	14			11	4		

p-values were calculated by Mann-Whitney *U* test.

Table 2
The relationship between miR-30c, MTDH and MUC1 expression in IMPC tissues.

IMPC								
	miR-30c		r_s	*p*	MTDH		r_s	*p*
	Low	High			Low	High		
MTDH			−0.221	0.013				
Low	29	15						
High	68	12						
MUC1			−0.3	<0.01			0.454	<0.01
Non-reversed patren	10	10			17	3		
Reversed patren	87	17			27	77		

p-values were spearman's rank correlation analysis.

4. Discussion

In the present study, for the first time, we demonstrated the important regulatory role of miR-30c in proliferation, metastasis and polarity reversal in IMPC. We found that miR-30c could negatively regulate MTDH expression by directly binding to its 3′UTR. MiR-30c/MTDH axis could inhibit cell proliferation, migration and invasion by targeting MTDH. MiR-30c/MTDH axis could also regulate the polarity reversal of tumor cell clusters in IMPC cells. Moreover, we revealed that miR-30c and MTDH were significantly associated with multiple clinical pathological characteristics, prognosis, and the 'inside-out' growth pattern of IMPC patients.

As an aggressive subtype of breast cancer, IMPC is characterized by a special growth pattern of tumor cell polarity reversal, invasion and metastasis [42,43]. Consistent with our previous study [9], 86 % of IMPC patients and 45 % of IDC-NST patients had lymph node metastasis, indicating a high lymph node metastasis rate in IMPC compared to IDC-NST. The prevalence of ER expression was 72 % and 60 % in IMPC and IDC-NST, respectively, comparable with previous reports by Chen AC and Tresserra F et al. [44,45].

MiR-30c can regulate multiple tumorigenesis processes by targeting variable genes [22,46,47]. But the underlying mechanism of miR-30c dysregulation in IMPC is unclear. Marchi C et al. showed that the genomic locations of miR-30c-1 and miR-30c-2, 1p34.2 and 6q13, respectively, were lost in IMPC [38]. The loss of chromatin regions may be responsible for the low expression of miR-30c in IMPC.

The dysregulation of MTDH is associated with several cancer-related processes, including cell proliferation, death, invasion, endothelial adhesion, metastasis and angiogenesis [27,48–50]. Hu et al. found that the MTDH genomic region 8q22 was frequently amplified in breast cancer, which led to MTDH overexpression, thereby promoting chemoresistance and metastasis of breast cancer patients with poor prognosis [49]. Genomic DNA deep sequencing results revealed that the entire 8q region was amplified in breast IMPC [51]. In the present study, by reporter assay and western blotting, we showed that miR-30c could target MTDH. Zhang et al. found that miR-30a could suppress proliferation, invasion and metastasis by targeting MTDH [50]. However, our previous real-time PCR results showed that only miR-30c (not miR-30a) was downregulated in IMPC compared with IDC-NST [23]. Using cell culture and xenograft models, the current research revealed that dysregulated miR-30c might post transcriptionally contribute to the overexpression of MTDH, thereby enhancing the aggressive characteristics of IMPC.

Loss of apico-basal polarity is recognized as an important factor in tumor development [52]. Several IMPC-specific genes and ontology pathways are involved in the regulation of cell polarity, adhesion and migration [53]. Accordingly, elucidation of the molecular mechanism of polarity reversion in IMPC may contribute to understanding the metastasis mechanism of breast cancer. MUC1 is localized to the external surface of the IMPC cell clusters, and has been described as an 'inside-out' growth pattern [42]. It might represent a more malignant phenotype when MUC1 staining patterns beyond apical localization [54]. MUC1 is also important in the initial attachment of carcinoma cells to tissues at distant sites to occur metastasis [55]. Our previous findings suggested that Sialyl Lewis X, an MUC1 epitope, might play an important role in lymph node metastasis in IMPC [43]. MTDH is also recruited during the maturation of the tight junction proteins ZO-1 and occludin in polarized epithelial cells [31], suggesting that MTDH is involved in cell polarity regulation. Overall, our study indicated that miR-30c negatively regulated MTDH, resulting in tumor cell cluster polarity reversal and might contribute to invasion and metastasis of IMPC.

In conclusion, we identified a miR-30c/MTDH mediated pathway that regulated proliferation, metastasis and polarity reversal of tumor cell clusters in IMPC. The components of this pathway represent attractive targets for the development of new therapeutic strategies in breast cancer, particularly in IMPC.

Availability of data and materials

Data associated with the study has not been deposited into a publicly available repository. Data are available from the corresponding author on reasonable request.

Ethics approval and consent to participate

The studies were approved by an independent ethics committee of the Department of Breast Cancer Pathology and Research Laboratory, Tianjin Medical University Cancer Hospital, Tianjin, China (Grant Nos. Ek2018136). All patients provided written

informed consent before study enrollment. All the steps/methods were performed in accordance with the relevant guidelines and regulations.

Financial Support

This work was supported by funding from the National Natural Science Foundation of China (Grant Nos. 82173344). Cancer Translational Medicine Seed Fund of Tianjin Medical University Cancer Institute and Hospital (Grant Nos.1804). Funded by Tianjin Key Medical Discipline (Specialty) Construction Project (Grant Nos.TJYXZDXK-012A).

Consent for publication

Not applicable.

CRediT authorship contribution statement

Yunwei Han: Writing – review & editing, Writing – original draft, Visualization, Validation, Supervision, Software, Resources, Project administration, Methodology, Investigation, Funding acquisition, Formal analysis, Data curation, Conceptualization. **Weidong Li:** Writing – review & editing, Writing – original draft, Validation, Supervision, Software, Resources, Methodology, Investigation, Data curation. **Renyong zhi:** Project administration, Methodology, Investigation, Formal analysis. **Gui Ma:** Software, Resources, Methodology, Formal analysis, Data curation. **Ang Gao:** Software, Resources, Methodology, Formal analysis, Data curation. **Kailiang Wu:** Resources, Methodology, Data curation. **Hui Sun:** Validation, Methodology, Formal analysis, Data curation. **Dan Zhao:** Validation, Project administration, Methodology, Investigation, Formal analysis. **Yiling Yang:** Supervision, Methodology, Investigation, Data curation. **Fangfang Liu:** Visualization, Resources, Methodology, Formal analysis. **Feng Gu:** Validation, Methodology, Formal analysis, Data curation. **Xiaojing Guo:** Validation, Supervision, Methodology, Investigation. **Jintang Dong:** Visualization, Validation, Software, Resources, Methodology, Funding acquisition, Formal analysis, Data curation. **Shuai Li:** Writing – review & editing, Writing – original draft, Visualization, Validation, Supervision, Resources, Methodology, Investigation, Data curation. **Li Fu:** Writing – review & editing, Validation, Project administration, Methodology, Investigation, Funding acquisition, Formal analysis, Data curation, Conceptualization.

Declaration of competing interest

The authors declare the following financial interests/personal relationships which may be considered as potential competing interests: Lifu reports was provided by none. Lifu reports a relationship with none that includes:. Lifu has patent none pending to none. none If there are other authors, they declare that they have no known competing financial interests or personal relationships that could have appeared to influence the work reported in this paper.

Acknowledgements

We thank Prof. Zhengmao Zhu, Ms. Liya Fu, Mr. Xing Fu Mr. Jun A, Mr. Mingcheng Liu, Ms. Qingxia Hu, Ms.Changying Fu, Ms. Ge Dong and Ms. Qiuying Li of Nankai University for helpful comments and assistance during the study.

Appendix A. Supplementary data

Supplementary data to this article can be found online at https://doi.org/10.1016/j.heliyon.2024.e33938.
Author contributions statement.

References

[1] S. Siriaunkgul, F.A. Tavassoli, Invasive micropapillary carcinoma of the breast, Mod. Pathol. 6 (1993) 660–662.
[2] WHO Classification of Tumors Editorial Board, WHO classification of tumors. Breast Tumors, fifth ed., IARC, Lyon, 2019.
[3] Y. Ohtsuki, N. Kuroda, S. Yunoki, S. Murakami, Y. Mizukami, Y. Okada, M. Iguchi, G.H. Lee, M. Furihata, Immunohistochemical analysis of invasive micropapillary carcinoma pattern in four cases of gastric cancer, Med. Mol. Morphol. 46 (2013) 114–121.
[4] M. Verdu, R. Roman, M. Calvo, N. Rodon, B. Garcia, M. Gonzalez, A. Vidal, X. Puig, Clinicopathological and molecular characterization of colorectal micropapillary carcinoma, Mod. Pathol. 24 (2011) 729–738.
[5] K. Koga, M. Hamasaki, F. Kato, M. Aoki, H. Hayashi, A. Iwasaki, H. Kataoka, K. Nabeshima, Association of c-Met phosphorylation with micropapillary pattern and small cluster invasion in pT1-size lung adenocarcinoma, Lung Cancer 82 (2013) 413–419.
[6] M. Paterakos, W.G. Watkin, S.M. Edgerton, D.H. Moore 2nd, A.D. Thor, Invasive micropapillary carcinoma of the breast: a prognostic study, Hum. Pathol. 30 (1999) 1459–1463.
[7] M.M. Walsh, I.J. Bleiweiss, Invasive micropapillary carcinoma of the breast: eighty cases of an underrecognized entity, Hum. Pathol. 32 (2001) 583–589.
[8] X. Guo, Y. Fan, R. Lang, F. Gu, L. Chen, L. Cui, G.A. Pringle, X. Zhang, L. Fu, Tumor infiltrating lymphocytes differ in invasive micropapillary carcinoma and medullary carcinoma of breast, Mod. Pathol. 21 (2008) 1101–1107.

[9] L. Chen, Y. Fan, R.G. Lang, X.J. Guo, Y.L. Sun, L.F. Cui, F.F. Liu, J. Wei, X.M. Zhang, L. Fu, Breast carcinoma with micropapillary features: clinicopathologic study and long-term follow-up of 100 cases, Int. J. Surg. Pathol. 16 (2008) 155–163.
[10] L. Fu, M. Ikuo, X.Y. Fu, T.H. Liu, T. Shinichi, [Relationship between biologic behavior and morphologic features of invasive micropapillary carcinoma of the breast], Zhonghua Bing Li Xue Za Zhi 33 (2004) 21–25.
[11] F. Liu, M. Yang, Z. Li, X. Guo, Y. Lin, R. Lang, B. Shen, G. Pringle, X. Zhang, L. Fu, Invasive micropapillary mucinous carcinoma of the breast is associated with poor prognosis, Breast Cancer Res. Treat. 151 (2015) 443–451.
[12] X. Guo, L. Chen, R. Lang, Y. Fan, X. Zhang, L. Fu, Invasive micropapillary carcinoma of the breast, Am. J. Clin. Pathol. 126 (2006) 740–746.
[13] J. Lv, Q. Shi, Y. Han, W. Li, H. Liu, J. Zhang, C. Niu, G. Gao, Y. Fu, R. Zhi, K. Wu, S. Li, F. Gu, L. Fu, Spatial transcriptomics reveals gene expression characteristics in invasive micropapillary carcinoma of the breast, Cell Death Dis. 12 (2021) 1095.
[14] Q. Shi, K. Shao, H. Jia, B. Cao, W. Li, S. Dong, J. Liu, K. Wu, M. Liu, F. Liu, H. Zhou, J. Lv, F. Gu, L. Li, S. Zhu, S. Li, G. Li, L. Fu, Genomic alterations and evolution of cell clusters in metastatic invasive micropapillary carcinoma of the breast, Nat. Commun. 13 (2022) 111.
[15] W. Li, Y. Han, C. Wang, X. Guo, B. Shen, F. Liu, C. Jiang, Y. Li, Y. Yang, R. Lang, Y. Fan, F. Gu, Y. Niu, X. Zhang, L. Zhang, H.Y. Wen, L. Fu, Precise pathologic diagnosis and individualized treatment improve the outcomes of invasive micropapillary carcinoma of the breast: a 12-year prospective clinical study, Mod. Pathol. 31 (2018) 956–964.
[16] Z. Yu, R. Baserga, L. Chen, C. Wang, M.P. Lisanti, R.G. Pestell, microRNA, cell cycle, and human breast cancer, Am. J. Pathol. 176 (2010) 1058–1064.
[17] Y.W. Kong, D. Ferland-McCollough, T.J. Jackson, M. Bushell, microRNAs in cancer management, Lancet Oncol. 13 (2012) e249–e258.
[18] G.A. Calin, C. Sevignani, C.D. Dumitru, T. Hyslop, E. Noch, S. Yendamuri, M. Shimizu, S. Rattan, F. Bullrich, M. Negrini, C.M. Croce, Human microRNA genes are frequently located at fragile sites and genomic regions involved in cancers, Proc Natl Acad Sci U S A 101 (2004) 2999–3004.
[19] L. Ma, J. Teruya-Feldstein, R.A. Weinberg, Tumour invasion and metastasis initiated by microRNA-10b in breast cancer, Nature 449 (2007) 682–688.
[20] J.H. Fang, Z.J. Zhang, L.R. Shang, Y.W. Luo, Y. Lin, Y. Yuan, S.M. Zhuang, Hepatoma cell-secreted exosomal microRNA-103 increases vascular permeability and promotes metastasis by targeting junction proteins, Hepatology 68 (2018) 1459–1475.
[21] J. Bockhorn, K. Yee, Y.F. Chang, A. Prat, D. Huo, C. Nwachukwu, R. Dalton, S. Huang, K.E. Swanson, C.M. Perou, O.I. Olopade, M.F. Clarke, G.L. Greene, H. Liu, MicroRNA-30c targets cytoskeleton genes involved in breast cancer cell invasion, Breast Cancer Res. Treat. 137 (2013) 373–382.
[22] J. Bockhorn, R. Dalton, C. Nwachukwu, S. Huang, A. Prat, K. Yee, Y.F. Chang, D. Huo, Y. Wen, K.E. Swanson, T. Qiu, J. Lu, S.Y. Park, M.E. Dolan, C.M. Perou, O. I. Olopade, M.F. Clarke, G.L. Greene, H. Liu, MicroRNA-30c inhibits human breast tumour chemotherapy resistance by regulating TWF1 and IL-11, Nat. Commun. 4 (2013) 1393.
[23] S. Li, C. Yang, L. Zhai, W. Zhang, J. Yu, F. Gu, R. Lang, Y. Fan, M. Gong, X. Zhang, L. Fu, Deep sequencing reveals small RNA characterization of invasive micropapillary carcinomas of the breast, Breast Cancer Res. Treat. 136 (2012) 77–87.
[24] G. Hu, Y. Wei, Y. Kang, The multifaceted role of MTDH/AEG-1 in cancer progression, Clin. Cancer Res. 15 (2009) 5615–5620.
[25] L. Wan, Y. Kang, Pleiotropic roles of AEG-1/MTDH/LYRIC in breast cancer, Adv. Cancer Res. 120 (2013) 113–134.
[26] L. Wan, G. Hu, Y. Wei, M. Yuan, R.T. Bronson, Q. Yang, J. Siddiqui, K.J. Pienta, Y. Kang, Genetic ablation of metadherin inhibits autochthonous prostate cancer progression and metastasis, Cancer Res. 74 (2014) 5336–5347.
[27] L. Wan, X. Lu, S. Yuan, Y. Wei, F. Guo, M. Shen, M. Yuan, R. Chakrabarti, Y. Hua, H.A. Smith, M.A. Blanco, M. Chekmareva, H. Wu, R.T. Bronson, B.G. Haffty, Y. Xing, Y. Kang, MTDH-SND1 interaction is crucial for expansion and activity of tumor-initiating cells in diverse oncogene- and carcinogen-induced mammary tumors, Cancer Cell 26 (2014) 92–105.
[28] N. Jariwala, D. Rajasekaran, J. Srivastava, R. Gredler, M.A. Akiel, C.L. Robertson, L. Emdad, P.B. Fisher, D. Sarkar, Role of the staphylococcal nuclease and tudor domain containing 1 in oncogenesis (review), Int J Oncol 46 (2015) 465–473.
[29] M. Shen, S. Xie, M. Rowicki, S. Michel, Y. Wei, X. Hang, L. Wan, X. Lu, M. Yuan, J.F. Jin, F. Jaschinski, T. Zhou, R. Klar, Y. Kang, Therapeutic targeting of metadherin suppresses colorectal and lung cancer progression and metastasis, Cancer Res. 81 (2021) 1014–1025.
[30] J.-y. Hao, Y.-l. Yang, F.-f. Liu, S. Li, W.-d. Li, X.-l. Qian, E. Paulos, L. Fu, MTDH expression in invasive micropapillary carcinoma of the breast, Clinical Oncology and Cancer Research (2011) 8.
[31] D.E. Britt, D.F. Yang, D.Q. Yang, D. Flanagan, H. Callanan, Y.P. Lim, S.H. Lin, D.C. Hixson, Identification of a novel protein, LYRIC, localized to tight junctions of polarized epithelial cells, Exp. Cell Res. 300 (2004) 134–148.
[32] R. Natrajan, P.M. Wilkerson, C. Marchio, S. Piscuoglio, C.K. Ng, P. Wai, M.B. Lambros, E.P. Samartzis, K.J. Dedes, J. Frankum, I. Bajrami, A. Kopec, A. Mackay, R. A'Hern, K. Fenwick, I. Kozarewa, J. Hakas, C. Mitsopoulos, D. Hardisson, C.J. Lord, C. Kumar-Sinha, A. Ashworth, B. Weigelt, A. Sapino, A.M. Chinnaiyan, C. A. Maher, J.S. Reis-Filho, Characterization of the genomic features and expressed fusion genes in micropapillary carcinomas of the breast, J. Pathol. 232 (2014) 553–565.
[33] K. Janik, M. Popeda, J. Peciak, K. Rosiak, M. Smolarz, C. Treda, P. Rieske, E. Stoczynska-Fidelus, M. Ksiazkiewicz, Efficient and simple approach to in vitro culture of primary epithelial cancer cells, Biosci. Rep. 36 (2016).
[34] M. Deng, H.L. Tang, X.H. Lu, M.Y. Liu, X.M. Lu, Y.X. Gu, J.F. Liu, Z.M. He, miR-26a suppresses tumor growth and metastasis by targeting FGF9 in gastric cancer, PLoS One 8 (2013) e72662.
[35] H. Tang, P. Liu, L. Yang, X. Xie, F. Ye, M. Wu, X. Liu, B. Chen, L. Zhang, miR-185 suppresses tumor proliferation by directly targeting E2F6 and DNMT1 and indirectly upregulating BRCA1 in triple-negative breast cancer, Mol Cancer Ther 13 (2014) 3185–3197.
[36] J. Li, N. Zhang, L.B. Song, W.T. Liao, L.L. Jiang, L.Y. Gong, J. Wu, J. Yuan, H.Z. Zhang, M.S. Zeng, M. Li, Astrocyte elevated gene-1 is a novel prognostic marker for breast cancer progression and overall patient survival, Clin. Cancer Res. 14 (2008) 3319–3326.
[37] B.V. Sinn, G. von Minckwitz, C. Denkert, H. Eidtmann, S. Darb-Esfahani, H. Tesch, R. Kronenwett, G. Hoffmann, A. Belau, C. Thommsen, H.J. Holzhausen, S. T. Grasshoff, K. Baumann, K. Mehta, M. Dietel, S. Loibl, Evaluation of Mucin-1 protein and mRNA expression as prognostic and predictive markers after neoadjuvant chemotherapy for breast cancer, Ann. Oncol. 24 (2013) 2316–2324.
[38] K.B. Horwitz, W.W. Dye, J.C. Harrell, P. Kabos, C.A. Sartorius, Rare steroid receptor-negative basal-like tumorigenic cells in luminal subtype human breast cancer xenografts, Proc Natl Acad Sci U S A. 105 (2008) 5774–5779.
[39] W. Yu, A. Datta, P. Leroy, L.E. O'Brien, G. Mak, T.S. Jou, K.S. Matlin, K.E. Mostov, M.M. Zegers, Beta1-integrin orients epithelial polarity via Rac 1 and laminin, Mol. Biol. Cell 16 (2005) 433–445.
[40] W. Yu, A.M. Shewan, P. Brakeman, D.J. Eastburn, A. Datta, D.M. Bryant, Q.W. Fan, W.A. Weiss, M.M. Zegers, K.E. Mostov, Involvement of RhoA, ROCK I and myosin II in inverted orientation of epithelial polarity, EMBO Rep. 9 (2008) 923–929.
[41] B. Liu, X. Zheng, F. Meng, Y. Han, Y. Song, F. Liu, S. Li, L. Zhang, F. Gu, X. Zhang, L. Fu, Overexpression of β1 integrin contributes to polarity reversal and a poor prognosis of breast invasive micropapillary carcinoma, Oncotarget 9 (2018) 4338–4353.
[42] Y.L. Yang, B.B. Liu, X. Zhang, L. Fu, Invasive micropapillary carcinoma of the breast: an Update, Arch. Pathol. Lab Med. 140 (2016) 799–805.
[43] J. Wei, L. Cui, F. Liu, Y. Fan, R. Lang, F. Gu, X. Guo, P. Tang, L. Fu, E-selectin and Sialyl Lewis X expression is associated with lymph node metastasis of invasive micropapillary carcinoma of the breast, Int. J. Surg. Pathol. 18 (2010) 193–200.
[44] A.C. Chen, A.C. Paulino, M.R. Schwartz, A.A. Rodriguez, B.L. Bass, J.C. Chang, B.S. Teh, Population-based comparison of prognostic factors in invasive micropapillary and invasive ductal carcinoma of the breast, Br. J. Cancer 111 (2014) 619–622.
[45] F. Tresserra, P.J. Grases, R. Fabregas, A. Fernandez-Cid, S. Dexeus, Invasive micropapillary carcinoma. Distinct features of a poorly recognized variant of breast carcinoma, Eur. J. Gynaecol. Oncol. 20 (1999) 205–208.
[46] S.S. Suh, J.Y. Yoo, R. Cui, B. Kaur, K. Huebner, T.K. Lee, R.I. Aqeilan, C.M. Croce, FHIT suppresses epithelial-mesenchymal transition (EMT) and metastasis in lung cancer through modulation of microRNAs, PLoS Genet. 10 (2014) e1004652.
[47] Y. Fang, H. Shen, Y. Cao, H. Li, R. Qin, Q. Chen, L. Long, X.L. Zhu, C.J. Xie, W.L. Xu, Involvement of miR-30c in resistance to doxorubicin by regulating YWHAZ in breast cancer cells, Braz. J. Med. Biol. Res. 47 (2014) 60–69.
[48] D.M. Brown, E. Ruoslahti Metadherin, A cell surface protein in breast tumors that mediates lung metastasis, Cancer Cell 5 (2004) 365–374.

[49] G. Hu, R.A. Chong, Q. Yang, Y. Wei, M.A. Blanco, F. Li, M. Reiss, J.L. Au, B.G. Haffty, Y. Kang, MTDH activation by 8q22 genomic gain promotes chemoresistance and metastasis of poor-prognosis breast cancer, Cancer Cell 15 (2009) 9–20.
[50] N. Zhang, X. Wang, Q. Huo, M. Sun, C. Cai, Z. Liu, G. Hu, Q. Yang, MicroRNA-30a suppresses breast tumor growth and metastasis by targeting metadherin, Oncogene 33 (2014) 3119–3128.
[51] C. Marchio, M. Iravani, R. Natrajan, M.B. Lambros, K. Savage, N. Tamber, K. Fenwick, A. Mackay, R. Senetta, S. Di Palma, F.C. Schmitt, G. Bussolati, L.O. Ellis, A. Ashworth, A. Sapino, J.S. Reis-Filho, Genomic and immunophenotypical characterization of pure micropapillary carcinomas of the breast, J. Pathol. 215 (2008) 398–410.
[52] S.I. Ellenbroek, S. Iden, J.G. Collard, Cell polarity proteins and cancer, Semin. Cancer Biol. 22 (2012) 208–215.
[53] N. Gruel, L. Fuhrmann, C. Lodillinsky, V. Benhamo, O. Mariani, A. Cedenot, L. Arnould, G. Macgrogan, X. Sastre-Garau, P. Chavrier, O. Delattre, A. Vincent-Salomon, LIN7A is a major determinant of cell-polarity defects in breast carcinomas, Breast Cancer Res. 18 (2016) 23.
[54] A. Siroy, F.W. Abdul-Karim, J. Miedler, N. Fong, P. Fu, H. Gilmore, J. Baar, MUC1 is expressed at high frequency in early-stage basal-like triple-negative breast cancer, Hum. Pathol. 44 (2013) 2159–2166.
[55] P. Ciborowski, O.J. Finn, Non-glycosylated tandem repeats of MUC1 facilitate attachment of breast tumor cells to normal human lung tissue and immobilized extracellular matrix proteins (ECM) in vitro: potential role in metastasis, Clin. Exp. Metastasis 19 (2002) 339–345.